SUPPLEMENTAL METHODS

Segmentation-Based Method with Bone Prediction (SEGwBONE)

Segmentation-based LACs are assigned to non-osseous regions in a dataset, whereas LACs for bone areas are computed using an approach based on atlas- and pattern recognition.

The MR data is segmented into the classes outer air, inner air, lungs, fat tissue, non-fat tissue, fat/non-fat tissue mixture. Fat and non-fat tissues as well as fat/non-fat tissue mixture are classified based on the Dixon fat and water images. Voxels in the fat images of more than twice the intensity of water are assigned to fat and vice versa; remaining voxels which are not subsequently assigned to air or lungs are considered as fat/non-fat tissue mixture. Lungs were detected by hierarchical clustering as a set of one or two regions of low intensity in the in-phase image. The remaining regions of low intensity inside the body were assigned to the class inner air. Morphological operations were applied to the inner part of the body contour to limit the propagation of potential susceptibility artifacts. The classes outer air/inner air, lungs, fat tissue, non-fat tissue and fat/non-fat tissue mixture are assigned predefined attenuation values (0 cm^{-1}, 0.024 cm^{-1}, 0.0856 cm^{-1}, 0.1007 cm^{-1} and 0.0988 cm^{-1}).

LACs for bone areas were determined as follows: In the first step, each segmented MR volume from the atlas database was non-rigidly registered to the segmented patient MR using Elastix *(10)* and the resulting transformations were applied to the corresponding CT images. Subsequently, areas of possible bone occurrence are determined by applying a bone/soft tissue threshold (LAC > 0.1106 cm^{-1}), on each co-registered atlas CT, followed by Gaussian filtering and a dilation operation. A patient-specific map of potential bone locations is then computed by averaging. LACs for voxels in these regions were then computed using Gaussian Process Regression. For each potential bone voxel, an LAC was predicted based on the spatially closest voxels from the co-registered images in the atlas database. Local neighborhood of the MR and segmented MR images is also matched,

allowing for a more patient-specific prediction. Finally, predicted LACs above the bone/soft tissue threshold are assigned to the corresponding voxels in the attenuation map.

Registration of CT to MR Datasets for Creation of the Pediatric Atlas Database

The CT datasets were preprocessed to remove ancillary objects as the patient table and fixing devices. An initial alignment was performed such that the lung centers of gravity for MR and CT datasets were matched. The in-phase, fat and water MR images were normalized for intensity variations and a segmented image was created, to which the CT was co-registered. The segmentation was analog to the method that was used to assign the non-bone regions for SEGwBONE. The registration was performed in three steps using the open source registration toolkit Elastix *(9)*. The initial registration step was rigid, followed by affine and non-rigid B-spline registration. A mask of valid voxels was used for the fixed MR image, such that arm regions were excluded. Normalized mutual information was used as registration metric. The grid spacing of the B-spline deformation field was set to 3.2 cm, which was previously empirically determined to yield a good compromise between robustness of registration and deformation flexibility. A 4-level multi-resolution schedule was used to reduce the probability of the registration finishing at a local optimum. Registration accuracy was verified visually via side-by side view and image fusion. Except regions in the upper thorax and extremities, which showed higher deviations due to large positional differences, we found the registration to be accurate.

SUPPLEMENTAL FIGURES

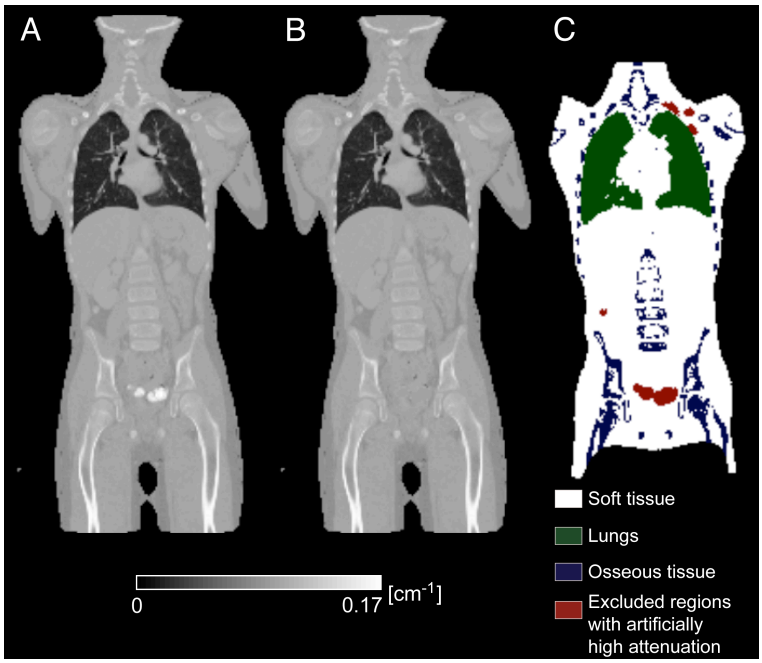

Supplemental Figure 1: A sample CT-based reference attenuation map before (A) and after the removal of artificially high HUs (B) as well as the region map used for evaluation of the atlas influence on attenuation map prediction quality (C). White regions were assigned to soft tissue, green regions to lung tissue and blue regions to bones. Regions that were excluded from evaluation due to injection of contrast agent are shown in red.

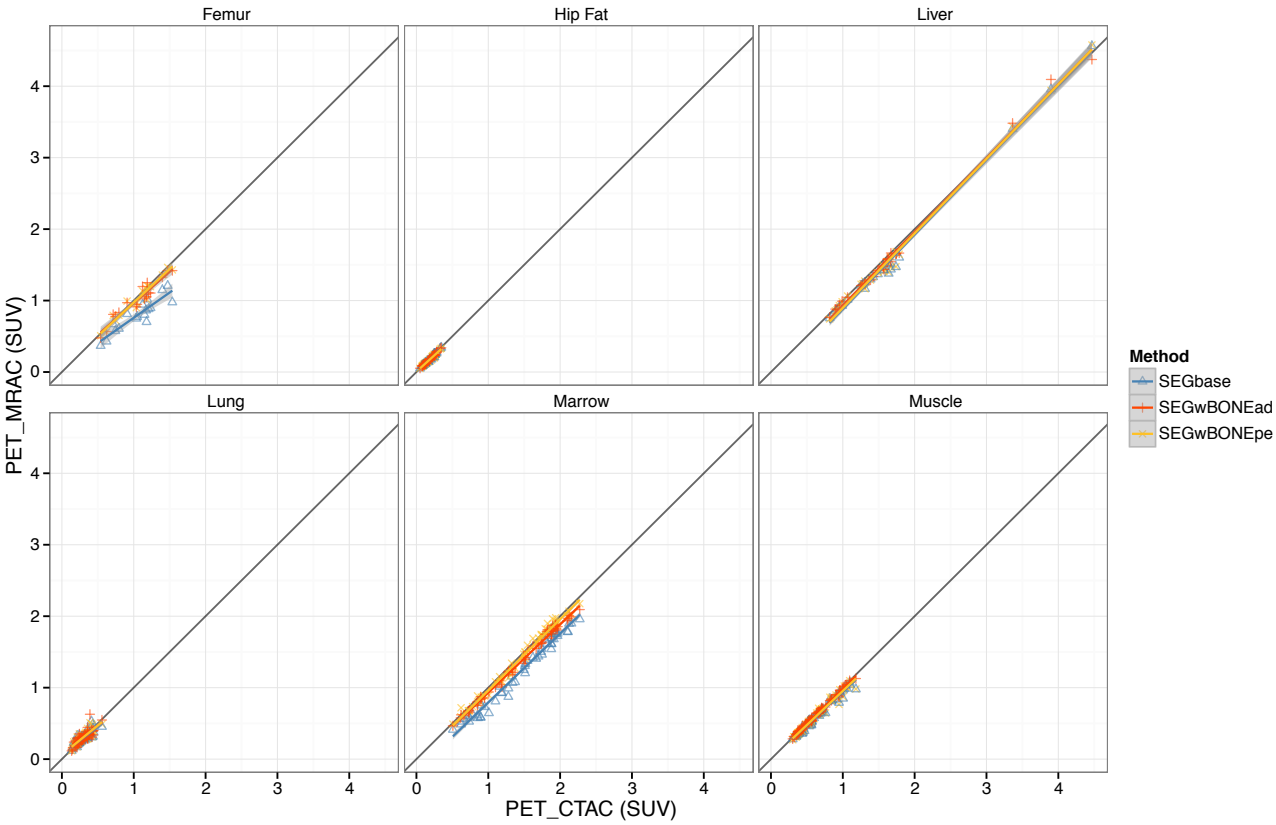

Supplemental Figure 2: Scatter plots of mean activity in VOIs with physiological uptake for PET images that were corrected for attenuation with MRAC and PET images corrected with reference CTAC. Black solid lines represent lines of identity; colored solid lines represent regression lines.

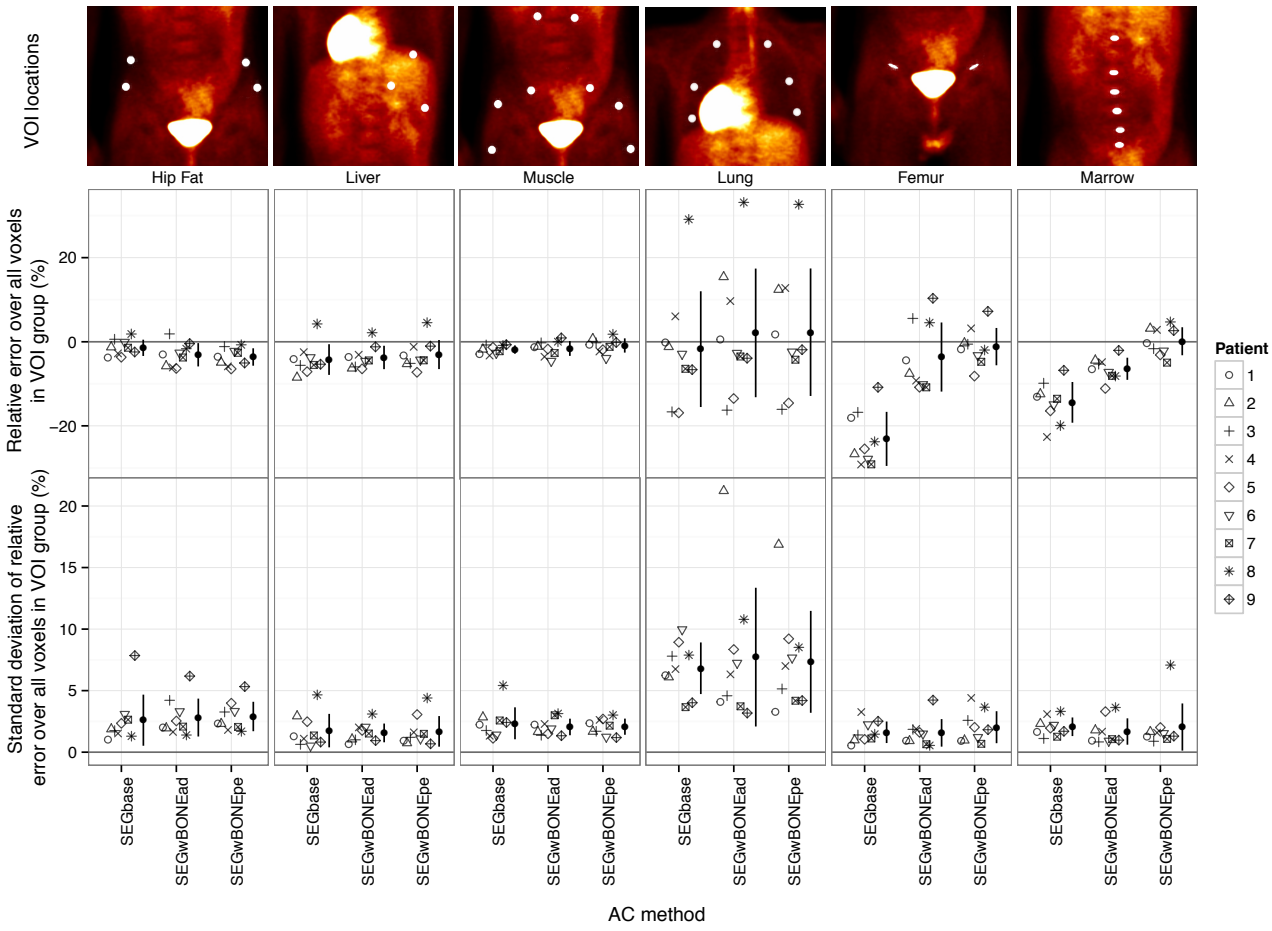

Supplemental Figure 3: Means (top row) and SDs (bottom row) of relative differences over all voxels in VOI category, computed for each patient. Voxel-wise relative differences were computed between PET_{MRAC} and PET_{CTAC} for groups of VOIs with physiological uptake.

SUPPLEMENTAL TABLES

Supplemental Table 1: Comparison of inter- and intra-patient variability of LACs for pediatric (n=17) and adult (n=16) patient collectives. SD of $Mean_{patient,group}$ over all patients in a collective indicates inter-patient variability. Mean of $SD_{patient,group}$ and relative $SD_{patient,group}$ indicates intra-patient variability. $Mean_{patient,group}$ and $SD_{patient,group}$ were computed over all voxels from VOIs in one tissue category for each patient.

VOI group	Patient collective	SD of $Mean_{patient,group}$ ($LAC*10^4$)	Mean of $SD_{patient,group}$ ($LAC*10^4$)	Mean of relative $SD_{patient,group}$ (%)
Hip fat	Pediatric	26.9	18.7	2.1
Hip fat	Adult	11.0	16.4	1.9
Liver	Pediatric	15.1	11.1	1.1
Liver	Adult	15.9	13.3	1.3
Muscle	Pediatric	2.6	14.1	1.4
Muscle	Adult	3.0	12.4	1.2
Lung	Pediatric	68.9	73.5	27.4
Lung	Adult	35.9	75.3	34.0
Femur	Pediatric	17.5	27.3	2.4
Femur	Adult	13.2	41.0	3.5
Marrow	Pediatric	22.5	20.5	1.9
Marrow	Adult	15.5	18.8	1.7

Supplemental Table 2: Parameters of regression coefficients of fit for VOIs with normal physiological uptake in PET images reconstructed with CTAC versus MRAC with the corresponding P values. P values of statistically significant coefficients are denoted in bold.

VOI	AC method	R^2	Slope	Intercept	P value of fit
Hip Fat	SEGbase	0.9928	0.9974	-0.0023	**<0.0001**
Hip Fat	SEGwBONEad	0.9939	0.9457	0.0028	**<0.0001**
Hip Fat	SEGwBONEpe	0.9921	0.9701	-0.0014	**<0.0001**
Liver	SEGbase	0.9905	1.0523	-0.1352	**<0.0001**
Liver	SEGwBONEad	0.9950	1.0333	-0.1040	**<0.0001**
Liver	SEGwBONEpe	0.9918	1.0519	-0.1172	**<0.0001**
Muscle	SEGbase	0.9952	0.9826	-0.0009	**<0.0001**
Muscle	SEGwBONEad	0.9951	0.9824	0.0011	**<0.0001**
Muscle	SEGwBONEpe	0.9948	1.0003	-0.0050	**<0.0001**
Lung	SEGbase	0.7740	0.7854	0.0547	**<0.0001**
Lung	SEGwBONEad	0.6746	0.8400	0.0501	**<0.0001**
Lung	SEGwBONEpe	0.7224	0.7981	0.0631	**<0.0001**
Femur	SEGbase	0.9197	0.7848	-0.0144	**<0.0001**
Femur	SEGwBONEad	0.9236	0.8822	0.0815	**<0.0001**
Femur	SEGwBONEpe	0.9686	0.9966	-0.0075	**<0.0001**
Marrow	SEGbase	0.9897	0.9395	-0.1008	**<0.0001**
Marrow	SEGwBONEad	0.9919	0.9547	-0.0240	**<0.0001**
Marrow	SEGwBONEpe	0.9900	0.9666	0.0442	**<0.0001**

Supplemental Table 3: Comparison of inter- and intra-patient variability of PET bias. SD of $Mean_{patient,group,ACmethod}$ over n=9 patients indicates inter-patient variability. Mean of $SD_{patient,group,ACmethod}$ indicates intra-patient variability. $Mean_{patient,group,ACmethod}$ and $SD_{patient,group,ACmethod}$ were computed for relative differences between PET_{MRAC} and PET_{CTAC} over all voxels from VOIs in one tissue category for each patient and each MRAC method.

VOI group	AC method	SD of $Mean_{patient,group,ACmethod}$ (%)	Mean of $SD_{patient,group,ACmethod}$ (%)
Hip fat	SEGbase	1.94	2.60
Hip fat	SEGwBONEad	2.77	2.81
Hip fat	SEGwBONEpe	2.07	2.80
Liver	SEGbase	3.65	1.75
Liver	SEGwBONEad	2.78	1.57
Liver	SEGwBONEpe	3.46	1.69
Muscle	SEGbase	0.99	2.35
Muscle	SEGwBONEad	1.77	2.05
Muscle	SEGwBONEpe	1.69	2.07
Lung	SEGbase	13.76	6.82
Lung	SEGwBONEad	15.29	7.72
Lung	SEGwBONEpe	15.17	7.34
Femur	SEGbase	6.43	1.62
Femur	SEGwBONEad	8.21	1.57
Femur	SEGwBONEpe	4.44	2.03
Marrow	SEGbase	4.84	2.06
Marrow	SEGwBONEad	2.63	1.68
Marrow	SEGwBONEpe	3.33	2.04